Polymer 122 (2017) 105–116

Contents lists available at ScienceDirect

Polymer

journal homepage: www.elsevier.com/locate/polymer

Study on the structure-properties relationship of biodegradable and biobased aliphatic copolyesters based on 1,3-propanediol, 1,4-butanediol, succinic and adipic acids

Thibaud Debuissy [a], Parveen Sangwan [b], Eric Pollet [a], Luc Avérous [a, *]

[a] BioTeam/ICPEES-ECPM, UMR CNRS 7515, Université de Strasbourg, 25 Rue Becquerel, 67087 Strasbourg Cedex 2, France
[b] CSIRO Manufacturing, Private Bag 10, Clayton South, Victoria, 3169, Australia

ARTICLE INFO

Article history:
Received 16 May 2017
Received in revised form
19 June 2017
Accepted 21 June 2017
Available online 22 June 2017

Keywords:
Copolyesters synthesis
Structure-properties relationship
Thermal property
Crystallization rate
Isodimorphism
Biodegradation

ABSTRACT

Two series of high molar mass biobased aliphatic copolyesters [poly(1,3-propylene succinate-*ran*-1,4-butylene succinate) (PPBS) and poly(1,3-propylene adipate-*ran*-1,4-butylene adipate) (PPBA) were synthesized with different 1,3-propanediol/1,4-butanediol (1,3-PDO/1,4-BDO) molar ratio by trans-esterification in melt, using titanium (IV) isopropoxide as catalyst. NMR, SEC, FTIR, WAXS, TGA and DSC analyses and aerobic biodegradation in soil measurements were used to fully characterize copolyesters. Their compositions were similar to the feed ones with random distribution of 1,3-PDO and 1,4-BDO segments along chains. Copolyesters exhibited an excellent stability until at least 275 °C with a degradation profile dependent only of the diacid structure. Moreover, the shortening of the diacid and diol lengths induced an increase of T_g and a decrease of the crystallization rate, especially with 1,3-PDO, until having amorphous copolyesters for 1,3-PDO content of 60–100 and 80 mol.% for PPBS and PPBA, respectively. Furthermore, both copolyesters showed an isodimorphic co-crystallization behavior characterized by a pseudo-eutectic melting behavior and the presence of only one crystalline phase, except for PPBA with 1,3-PDO content of 50–59 mol.% which were in molten state. Lastly, the aerobic biodegradation rate in soil increased with the increase of the diacid length from succinic to adipic acids and the diol length from 1,3-propanediol to 1,4-butanediol monomers without showing any residual ecotoxicity.

1. Introduction

Over the last decades, renewable polymers as an alternative to petroleum-based materials have attracted considerable attention from both academic and industrial groups. These biobased polymers can also present new macromolecular architectures with advanced properties [1]. Among them, poly(hydroxyalkanoate)s [2], poly(lactic acid) [3], poly(butylene succinate) (PBS) [4] have seen their interest and industrial productions growing for various fields *e.g.*, on packaging, agriculture, biomedical applications or sanitary.

Till recently, biobased 1,3-propanediol (1,3-PDO) was not available in the market at low cost with sufficient purity for chemical purposes. These disadvantages have been lately overcome by the development of new bioprocesses permitting an increase of the industrial production using biochemical pathways, mainly from glycerol [5,6]. The development of biorefineries around the world was a strong input on the production of biobased 1,3-PDO from different producers. Indeed, biorefineries permit the large bioproduction of a wide range of biobased building blocks, such as 1,4-butanediol (1,4-BDO), succinic acid (SA), adipic acid (AA) … [7,8] 1,4-BDO is a short diol which can now be industrially produced *via* a chemical process of hydrogenation from SA [7,9]. However, recently Genomatica has genetically modified *E. Coli* to obtain the straight bioproduction of 1,4-BDO from sugars [10]. Now industrially available, biobased 1,4-BDO can be largely used in polycondensation or polyaddition reactions for the synthesis of polyurethanes [11], polyesters [12,13] and polyamides [12]. Biobased SA, listed by the US-DoE as one of the strategic platform chemicals from renewable resources [8,9,14], has seen its interest growing for the production of various polymers with different chemical structures such as polyesters, polyamides … [8,15]. AA is another aliphatic dicarboxylic acid which is also used for the synthesis of polyamides, polyurethanes and polyesters [12,13,15].

* Corresponding author.
E-mail address: luc.averous@unistra.fr (L. Avérous).

http://dx.doi.org/10.1016/j.polymer.2017.06.045
0032-3861/

Recently, new biological pathways were discovered for the direct bioproduction of AA from different biomass [16].

Aliphatic polyesters based on these four different building blocks have been developed and especially SA-based (co)polyesters [13,15,17]. PBS for instance, is one of the aliphatic polyesters with highest melting temperature (T_m of 113 °C) and excellent mechanical properties, comparable with those of conventional petroleum-based polymers, such as polyolefins. PBS became, thus, a promising candidate to replace common polymers with a growing production level during the last decade [18].

Developed from both academic and industrial perspectives, aliphatic polyesters based on 1,3-PDO have also attracted increasing interest since two decades, due to their excellent properties. For instance, poly(1,3-propylene terephthalate) (PPT), one of the most studied 1,3-PDO-based polyesters, is commercially available (Sorona®, Dupont) since a decade [19,20]. Because of the odd number of methylene groups in 1,3-PDO, PPT chains have a more angular structure than the conventional poly(1,2-ethylene terephthalate) (PET) or poly(1,4-butylene terephthalate) (PBT) leading to PPT fibers showing a higher resilience and stress recovery than PET or PBT [21]. However, PPT as well as PET or PBT are not biodegradable.

Recently, several renewable and biodegradable aliphatic polyesters based on 1,3-PDO such as poly(1,3-propylene succinate) (PPS), poly(1,3-propylene glutarate), poly(1,3-propylene adipate) (PPA) and poly(1,3-propylene azelate) have been studied [22–25]. In addition, different copolyesters as a route to prepare tailor-made aliphatic copolyesters with improved properties were investigated, such as poly(caprolactone-*block*-1,3-propylene adipate) [26], poly(1,2-ethylene succinate-*co*-1,3-propylene succinate) [27] and poly(1,3-propylene succinate-*co*-1,3-propylene adipate) (PPSA) [28].

Besides, poly(1,3-propylene succinate-*co*-1,4-butylene succinate) (PPBS) copolyesters has been broadly studied in connection to the remarkable properties of both corresponding homopolyesters (*i.e.* PPS and PBS) [29–34]. Papageorgiou and Bikiaris showed that the addition of 1,3-PDO to PBS significantly decreased the T_m and the degree of crystallinity leading to an increase of the biodegradation rate [29]. Moreover, the T_g of PPBS non-linearly increased with the 1,3-PDO content [31] and a change of the crystalline structure of copolyesters was observed for high 1,3-PDO content [29]. Finally, the Young modulus increased with the 1,3-PDO content whereas the tensile strength decreased [29]. Nevertheless, none of previous studies paid attention to the possible isodimorphic co-crystallization behavior of PPBS as it was highlighted for other aliphatic copolyesters [35,36]. For its part, the poly(1,3-propylene adipate-*co*-1,4-butylene adipate) (PPBA) copolyesters, which possesses a close structure to PPBS, had never been studied. The higher chain length of AA building blocks compared to SA could provide higher flexibility to the copolyester and, thus, counteract the poor crystallization rate of 1,3-PDO for example.

The aim of the study was, first, to synthesize high molar mass PPBS and PPBA copolyesters with various 1,3-PDO/1,4-BDO ratios using the transesterification polycondensation reaction process from the melt with an efficient titanium-based organometallic catalyst [13,22,29]. Then, in depth chemical and physico-chemical analyses of the different synthesized macromolecular architectures were performed. The molar mass and the chemical architectures of copolyesters were determined by SEC, ^{1}H-, ^{13}C-, ^{31}P NMR and FTIR. The crystalline structure, thermal stability and thermal properties were analyzed by WAXS, TGA and DSC, respectively. The biodegradation rate in soil was investigated according to international standard test method (ISO 17556:2012). The effect of the 1,3-PDO/1,4-BDO molar composition and the diacid (SA or AA) used on copolyesters properties was particularly discussed.

2. Experimental part

2.1. Materials

Biobased succinic acid (SA) (99.5%) was kindly supplied by BioAmber (France). SA was bioproduced by fermentation of glucose (from wheat or corn) and obtained after a multistep process based on several purifications, evaporation and crystallization stages. 1,4-BDO (99%), methanol (≥99.6%), chloroform (99.0–99.4%), chromium(III) acetyl acetonate (97%), 2-chloro-4,4,5,5-tetramethyl-1,3,2-dioxaphospholane (Cl-TMDP, 95%) and cholesterol (>99%) were purchased from Sigma-Aldrich. 1,3-propanediol (1,3-PDO) (98%) and pyridine HPLC grade (99.5+%) were purchased from Alfa Aesar. Adipic acid (AA) (99%), titanium (IV) isopropoxide (TTIP) (98+%) and extra dry toluene (99.85%) were supplied by Acros. All reactants were used without further purification. All solvents used for the analytical methods were of analytical grade.

2.2. Synthesis of copolyesters

Aliphatic copolyesters were synthesized by a two-stage melt polycondensation method (esterification and transesterification). Syntheses are performed in a 50 mL round bottom flask with a distillation device to remove by-products of the reaction (mainly water). All reactions were performed with a diol/acid molar ratio of 1.1/1. For each reaction, 10.0 g of diacid (SA or AA) were used and the weight of diols was adjusted according to the composition. During the first step (esterification), the reaction mixture was maintained under a constant argon flux and magnetically stirred at 300 rpm. The reactor temperature was set to 190 °C for 3 h. After 3 h of oligomerization, the remaining by-products of the reaction was distilled off by reducing the pressure to 200 mbar for 5 min, and then the proper amount (0.1 mol.% of TTIP *vs.* the amount of diacid used) of a 5 wt% solution of TTIP in extra dry toluene was introduced inside the reactor under a constant argon flux. The reaction mixture was heated to 210 °C for 45 min. In the second step (transesterification), the reactor temperature was slowly increased to 230 °C and the pressure was decreased stepwise over period of 5 min at 100, 50 and 25 mbar to avoid excessive foaming and to minimize oligomer sublimation (a potential problem during the melt polycondensation). The transesterification continued for 3–4 h. The global reaction procedure is summarized in Scheme 1. To end, the synthesized polyester was cooled down, dissolved in chloroform, and precipitated into a large volume of vigorously stirred dry ice-cold methanol. Thereafter, the precipitate was filtered with a fine filter (0.45 μm), washed with cold methanol and dried under reduced pressure in an oven at 40 °C, for 24 h. Lightly colored (ivory white or pale yellow) (co)polyesters were finally obtained.

Different poly(1,3-propylene succinate-*co*-1,4-butylene succinate) (PPBS) and poly(1,3-propylene adipate-*co*-1,4-butylene adipate) (PPBA) were synthesized with various 1,3-PDO/1,4-BDO molar ratios (100/0, 80/20, 60/40, 50/50, 40/60, 20/80 and 0/100). Samples are denoted "PPxByS" or "PPxByA" with x and y as the molar proportion of 1,3-PDO and 1,4-BDO (determined by ^{1}H NMR), respectively. Then, the four basic homopolyesters ($PP_{100}B_0S$, $PP_0B_{100}S$, $PP_{100}B_0A$ and $PP_0B_{100}A$) can also be denoted as PPS, PBS, PPA and PBA, respectively.

2.3. General methods and analysis

^{1}H- and ^{13}C NMR spectra were obtained with a Bruker 400 MHz spectrometer. $CDCl_3$ was used as solvent to prepare solutions with concentrations of 8–10 and 30–50 mg/mL for ^{1}H NMR and ^{13}C NMR, respectively. The number of scans was set to 128 for ^{1}H NMR

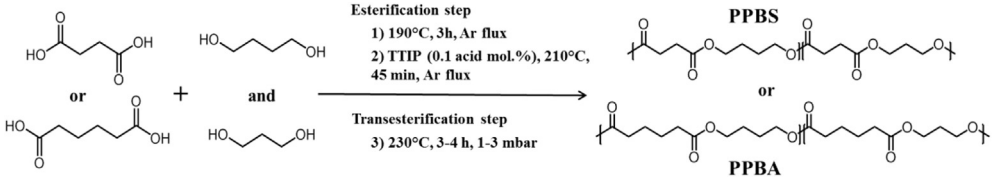

Scheme 1. Reaction procedure of PPBS and PPBA copolyesters.

and at least 4000 for ^{13}C NMR. Calibration of the spectra was performed using the specific $CDCl_3$ peak (δ_H = 7.26 ppm, δ_C = 77.16 ppm).

^{31}P NMR was performed after phosphitylation of the samples, according to standard protocols [12,37]. Spectra were obtained on a Bruker 400 MHz spectrometer (256 scans at 20 °C). All chemical shifts reported are relative to the reaction product of water with Cl-TMDP, which gives a sharp signal in pyridine/$CDCl_3$ at 132.2 ppm. The quantitative analysis of end-groups and the calculation of molar masses by ^{31}P NMR were performed based on previous reports [13,37].

Size exclusion chromatography (SEC) was performed to determine the number-average molar mass (M_n), the mass-average molar mass (M_w) and the dispersity (Đ) of the samples. A Shimadzu liquid chromatograph was equipped with PLGel Mixed-C and PLGeL 100 Å columns and a refractive index detector. Chloroform was used as eluent at a flow rate of 0.8 mL/min. The apparatus was calibrated with linear polystyrene standards from 162 to 1,650,000 g/mol.

Infrared spectroscopy (IR) was performed with a Nicolet 380 Fourier transformed infrared spectrometer (Thermo Electron Corporation) used in reflection mode and equipped with an ATR diamond module (FTIR-ATR). The FTIR-ATR spectra were collected at a resolution of 4 cm^{-1} and with 64 scans per run.

Differential scanning calorimetry (DSC) was performed using a TA Instrument Q 200 apparatus under nitrogen (flow rate of 50 mL/min), calibrated with high purity standards. Samples of 2–3 mg were sealed in aluminum pans. A three-step procedure with a 10 °C/min ramp was applied that involved: (1) heating up from room temperature to 140 and 90 °C for PPBS and PPBA, respectively, and holding for 3 min to erase the thermal history, (2) cooling down to −80 °C and holding for 3 min and (3) heating (second heating) from −80 °C to the same temperature as the first heating. To determine the glass transition temperature (T_g), (co)polyesters samples in pans were melted at 130 °C, quickly quenched in liquid nitrogen in order to obtain fully amorphous (co)polyesters and then heated from −80 to 0 °C at 10 °C/min. DSC analyses were repeated three times for each sample. The degree of crystallinity (X_c) is calculated according to Equation (1),

$$X_c(\%) = \frac{\Delta H_m}{\Delta H_m^0} \times 100 \quad (1)$$

where ΔH_m is the melting enthalpy and ΔH_m^0 is the melting enthalpy of a 100% pure crystalline polyester.

Thermal degradations were studied by thermogravimetric analyses (TGA). Measurements were conducted under helium atmosphere (flow rate of 25 mL/min) using a Hi-Res TGA Q5000 apparatus from TA Instruments. Samples (1–3 mg) were heated from room temperature up to 600 °C at a rate of 20 °C/min. Isothermal degradation was performed for 2 h at 230 °C under a helium atmosphere.

Wide angle X-ray Scattering (WAXS) data were recorded on a Siemens D5000 diffractometer using Cu K_α radiation (1.5406 Å) at 25–30 °C in the range of 2θ = 14–34° at 0.4° min^{-1}.

2.4. Ester function density

The ester function density of polyesters is defined by the number of ester function by repetitive unit on the number of carbons in the main chain by repetitive unit. The ester function density of PPBA copolyesters ($D_{ester,\ copo,PPBA}$) is given by Equation (2),

$$D_{ester,copo,PPBA} = \chi_{1,3-PDO} \times D_{ester,PPA} + \chi_{1,4-BDO} \times D_{ester,\ PBA} \quad (2)$$

where: $\chi_{1,3\text{-PDO}}$ and $\chi_{1,4\text{-BDO}}$ are the 1,3-PDO and 1,4-BDO molar contents in the copolyester, $D_{ester,PPA}$ and $D_{ester,PBA}$ are the ester function density in PPA and PBA, respectively. The ester function density of PPBS copolyesters ($D_{ester,\ copo,PPBS}$) is defined by the same method.

2.5. Aerobic biodegradation study

Soil samples were collected from a biodynamic vineyard located in Mornington Peninsula (Victoria, Australia), and sieved using a screen size of 8 mm to obtain a homogeneous mix. Soil pH was 5.6 and moisture content approximately 38%.

Prior to the testing, the film samples were reduced in size to achieve approximately 2 cm × 2 cm maximum surface area of each individual piece of the test material. Each test material was tested in duplicate including the blank (the soil only) and positive reference (a mixture of cellulose and soil). The contents of all bioreactors were mixed and placed inside an in-house built respirometer unit [38]. The temperature was maintained at 30 ± 2 °C for a period of 180 days. Aerobic conditions were maintained by providing continuous supply of sufficient airflow to the vessels (70–80 mL/min). The amount of CO_2 generated in each bioreactor was measured (at least twice a day) using an infrared CO_2 analyzer and values were data logged into the computer. Theoretical amount of carbon dioxide ($THCO_2$), in grams per bioreactor, that the test and reference material can produce, was assessed and the degree of biodegradability (D_t), was calculated (for the test and reference materials) using Equation (3),

$$D_t = \frac{(CO_2)_T - (CO_2)_B}{THCO_2} \times 100 \quad (3)$$

where $(CO_2)_T$ is the cumulative amount of carbon dioxide evolved in each bioreactor containing test material (in grams per bioreactor); $(CO_2)_B$ is the mean cumulative amount of carbon dioxide evolved in the blank vessel (in grams per bioreactor).

Following this step, the cumulative amount of carbon dioxide evolved as a function of time and a curve of percentage biodegradation as a function of time were plotted. Mean values were calculated from the replicate bioreactors and used for plotting the curves. The test was terminated after duration of 180 days.

3. Results and discussion

3.1. Characterization of the copolyesters macromolecular architectures

Several PPBS and PBBA copolyesters were synthesized following a two-step melt polycondensation pathway (Scheme 1). In the first one, the reaction led to the formation of oligomers (M_n of about 2–3 kg/mol after 3 h of esterification) necessary to avoid any removal phenomenon (*e.g.* monomer sublimation) during the next step. In the second one, the transesterification of previously synthesized oligomers using titanium isopropoxide (TTIP) resulted in a significant increase of molar masses as shown in Fig. SI1. The molar masses of synthesized (co)polyesters determined by SEC are presented on Table 1. Synthesized polymers could be considered as high molar mass polyesters since these samples have $M_{n,SEC}$ higher than 20 kg/mol, with a dispersity (Đ) of about 1.6–1.9. Đ values were lower than the expected value of 2, surely due to a small loss of short oligomers during the precipitation step, even if this last process was performed with a maximum care (small filter and dry ice cold methanol) to recover the maximum of short chains. Indeed, polymerization yields determined after precipitation were rather high and varied in a very narrow range, close to 90%.

The final chemical structure and microstructure of PPBS and PPBA copolyesters was verified by ^{1}H-, ^{13}C-, ^{31}P NMR and FTIR. The ^{1}H NMR spectra of $PP_{50}B_{50}A$ and $PP_{50}B_{50}S$ copolyesters, as an example, are presented in Fig. 1-a and Fig. SI2, respectively. On the ^{1}H NMR spectra of PPBA, the two close signals at $\delta = 4.14$ and 4.18 ppm respectively assigned to O-C<u>H$_2$</u>-CH$_2$- protons from 1,4-BDO and 1,3-PDO units confirmed the presence of ester functions. Other ^{1}H chemical signals at $\delta = 1.65$, 1.70, 1.96 and 2.32 ppm were ascribed to CO-CH$_2$-C<u>H$_2$</u>- protons from adipate units, to O-CH$_2$-C<u>H$_2$</u>- protons from 1,4-BDO units, to O-CH$_2$-C<u>H$_2$</u>- protons from 1,3-PDO units and to CO-CH$_2$-C<u>H$_2$</u>- protons from adipate units, respectively. Interestingly, the hydroxyl (HO-C<u>H$_2$</u>-) end-group signal was detected at tiny intensity at $\delta = 3.67$ ppm, in compliance with the relatively high chain length of copolyesters. ^{1}H chemical shifts of succinate in PPBS were observed at $\delta = 1.70$ and 2.62 ppm assigned to CO-CH$_2$-C<u>H$_2$</u>- and CO-C<u>H$_2$</u>-CH$_2$- protons, respectively. The molar composition (1,3-PDO/1,4-BDO) of copolyesters was determined from ^{1}H NMR using propylene and butylene signals at $\delta = 4.14$ and 4.18 ppm, respectively (more details in SI.3). Determined 1,3-PDO and 1,4-BDO contents in the chains are given in Table 1. All synthesized copolyesters presented 1,3-PDO/1,4-BDO molar ratio similar to the initial feed ones, because of (i) the close esterification rate of both diols with AA and SA for non-catalyzed systems [39], (ii) our choice to perform the esterification step 20 °C below the 1,3-PDO boiling point (about 210 °C) to avoid monomer loss and (iii) the sufficient time of the first step to permit the synthesis of oligomers of enough length to avoid product loss.

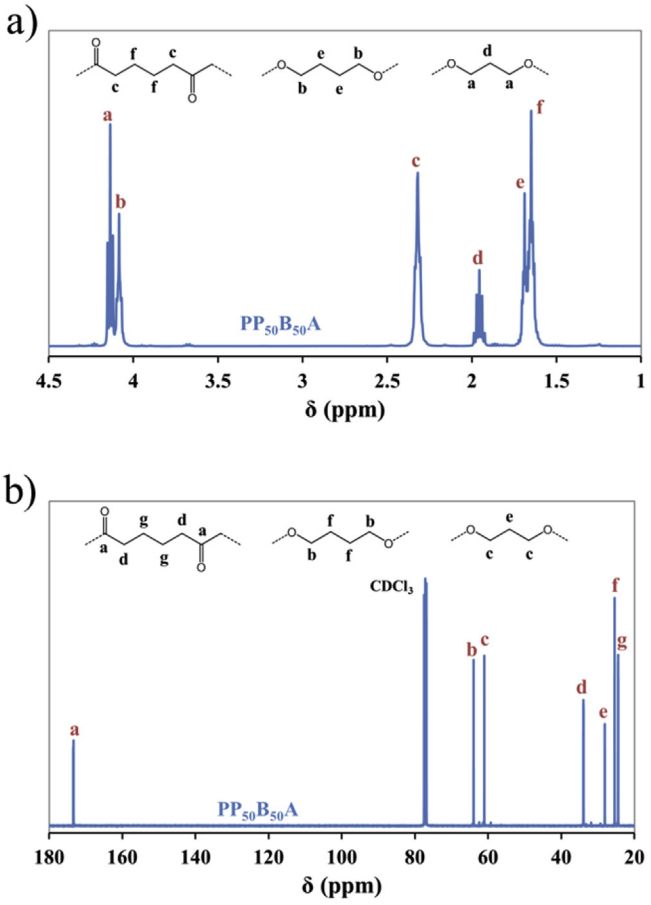

Fig. 1. (a) ^{1}H- and (b) ^{13}C NMR spectra of $PP_{50}B_{50}A$ copolyester.

^{13}C NMR was performed to investigate in detail the copolyester microstructure. ^{13}C NMR spectra of $PP_{50}B_{50}A$ and $PP_{50}B_{50}S$

Table 1
Main characterizations data of PPBS and PPBA copolyesters and the corresponding homopolymers.

Sample	Feed composition 1,3-PDO/1,4-BDO mol.%	^{1}H NMR	SEC		^{13}C NMR			^{31}P NMR		
		Exp. composition 1,3-PDO/1,4-BDO mol.%	M_n kg/mol	Đ	L_{PS} (or L_{PA})	L_{BS} (or L_{BA})	R	M_n kg/mol	OH end-groups %	COOH end-groups %
PPS	100/0	100/0	35.1	1.7	–	–	–	15.5	88	12
$PP_{80}B_{20}S$	80/20	79.6/20.4	31.7	1.7	4.1	1.4	0.96	14.4	76	24
$PP_{60}B_{40}S$	60/40	60.3/39.7	32.9	1.9	2.6	1.7	0.98	16.0	81	19
$PP_{50}B_{50}S$	50/50	49.5/50.5	29.8	1.8	2.0	2.1	0.98	14.1	82	18
$PP_{41}B_{59}S$	40/60	40.8/59.2	23.7	1.6	1.7	2.4	1.00	8.6	87	13
$PP_{21}B_{79}S$	20/80	20.8/79.2	38.6	1.7	1.3	4.9	0.98	13.7	38	62
PBS	0/100	0/100	39.2	1.7	–	–	–	17.3	78	22
PPA	100/0	100/0	29.4	1.7	–	–	–	10.1	77	23
$PP_{79}B_{21}A$	80/20	78.9/21.1	29.4	1.7	4.3	1.3	1.01	10.8	94	6
$PP_{59}B_{41}A$	60/40	59.3/40.7	20.0	1.6	2.5	1.6	1.04	7.9	94	6
$PP_{50}B_{50}A$	50/50	49.5/50.5	29.7	1.6	2.0	2.1	0.98	11.0	66	34
$PP_{40}B_{60}A$	40/60	39.7/60.3	35.2	1.6	1.6	2.6	1.00	13.7	65	35
$PP_{21}B_{79}A$	20/80	21.0/79.0	34.9	1.8	1.3	4.5	1.02	12.2	63	37
PBA	0/100	0/100	33.3	1.8	–	–	–	13.6	79	21

copolyesters are presented in Fig. 1-b and Fig. SI3, respectively. The details of ^{13}C chemical shifts are presented in SI.4. The copolyester microstructures (PAP, PAB and BAB triads for PPBA; PSP, PSB and BSB triads for PPBS), presented in Fig. 2-a and Fig. SI4 (with P, B, S and A as the 1,3-PDO, 1,4-BDO, SA and AA unit, respectively), were determined. For the PPBA copolyester, adipate units are present in all three triads and give distinctly different peaks with chemical shifts close to the ones of PPA or PBA for the CO-$\underline{CH_2}$-CH_2- carbons of adipate at δ ~34 ppm. Such results, with the splitting of the two signals (carbon atoms d_1, d_2, d_3 and d_4 in Fig. 2), enable the calculation of the average sequence length of PA and BA units (L_{PA} and L_{BA}, respectively) and the degree of randomness (R) using Equations (SI.3) to (SI.5). The same method was used in the case of PPBS, but the integration was performed using $\underline{CO}$-CH_2- carbons of succinate at δ ~172 ppm (Fig. SI4). Main data are listed in Table 1. According to the 1,3-PDO/1,4-BDO ratio, L_{PA} and L_{BA} for PPBA copolyesters (or L_{PS} and L_{BS}) varied between 1.3 and 4.8. R is equal to 1 for fully random copolymers [40]. R values in Table 1 show that we are precisely in this case for PPBA and PPBS copolyesters, composed of both diols, as it was expected by using a titanium-based organometallic catalyst [13,34].

^{31}P NMR analysis of PPBA and PPBA copolyesters was performed in $CDCl_3$ with cholesterol as standard. ^{31}P NMR spectra of copolyesters are presented in Fig. SI5 and SI6. All copolyesters showed primary hydroxyl (OH) (147.2–147.4 ppm) and carboxylic acid (COOH) (134.9 ppm) end-groups. The large majority of end-groups were OH groups surely due to the excess of OH functions initially introduced in the reaction mixture. Interestingly, 1,3-PDO (147.38 ppm) and 1,4-BDO (147.25 ppm) OH end-groups signals were separated in ^{31}P NMR spectra (Fig. SI7). The proportion of 1,3-PDO end-groups seemed to be slightly superior to the global 1,3-PDO content for all copolyesters (Table SI1), which is quite surprising since the transesterification led to random structures. One can suppose that this small difference could come from measurement uncertainty and the possible difference of stability of both modified hydroxyl end-groups with the phosphorus reactant [41].

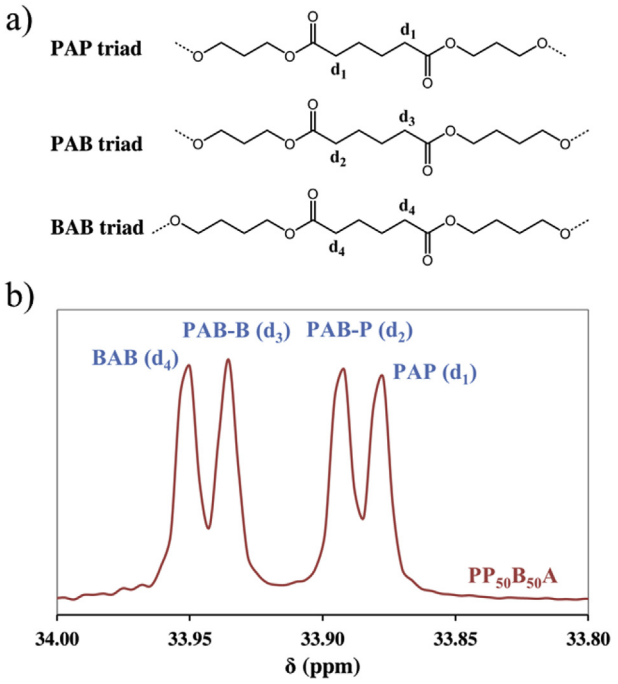

Fig. 2. (a) Possible triads for PPBA copolyesters, (b) ^{13}C NMR spectra of PPBA centered at δ ~ 34 ppm.

The molar masses of copolyesters determined by ^{31}P NMR ($M_{n,NMR}$) were lower compared to the one obtained by SEC, the latter being overestimated partly due to the calibration based on PS standards. $M_{n,NMR}$ varied between 8 and 17 kg/mol. Moreover, for the PBS and PBA samples, by using the Mark-Houwink-Sakurada (MHS) equation and parameters (K and a) from Charlier et al. [42] and Munari et al. [43], the calculated MHS-corrected M_n of PBS and PBA were 18.7 and 13.0 kg/mol, respectively. These results were close to the value determined by ^{31}P NMR (*i.e.*, 17.3 and 13.6 kg/mol). In conclusion, as observed for poly(butylene succinate-*co*-butylene adipate) (PBSA) copolyesters [13], $M_{n,NMR}$ gave a good estimation of a more accurate molar mass of copolyesters, even if this method based on the quantification of end-groups did not take into account the possible macrocycles that could have been produced during the polyester synthesis but which are not detectable by ^{31}P NMR analysis [13,42].

FTIR spectra of homopolyesters are presented in Fig. 3, whereas FTIR spectra of all PPBS and PPBA copolyesters are shown in Figs. SI8 and SI.9, respectively. First, strong signals at 1715-1725 cm^{-1} and 1150-1160 cm^{-1} respectively assigned to the C=O and -COO- asymmetric stretching vibrations demonstrated the presence of ester linkages. Then, the absence of broad signals around 3200-3500 cm^{-1} from COOH and OH end-groups confirmed the long chain length of (co)polyesters. Moreover, the presence of adipate segments instead of succinate segments shifted C=O stretching vibrations from 1715 to 1725 cm^{-1}, -CH_2- rocking vibrations from 805 to 735 cm^{-1} and -CO- stretching vibration from 1320 to 1255 cm^{-1}, respectively. Moreover, the intensity of the -CH_2- vibration signal at 2870-2970 cm^{-1} seemed to increase with the number of -CH_2- by repetitive units (for homopolyesters). Finally, few minor modifications of FTIR spectra were observed by increasing the 1,3-PDO content in PPBS and PPBA (more details in SI.7).

3.2. Thermal degradation

Thermal stability of PPBS and PPBA copolyesters was determined from TGA analyses performed under helium. The mass loss curves of PPBS and PPBA samples with their derivatives (DTG) curves are plotted in Fig. 4, whereas the corresponding data are reported in Table SI2. At temperature below 260 °C, all samples appeared to be stable. All copolyesters degraded in two main steps involving competitive mechanisms. A small mass loss (<5%) was first observed at 260–315 °C and 270–325 °C for PPBS and PPBA copolyesters, respectively. This mass loss was due to the degradation of the shortest polyester chains [12]. Then, a major degradation

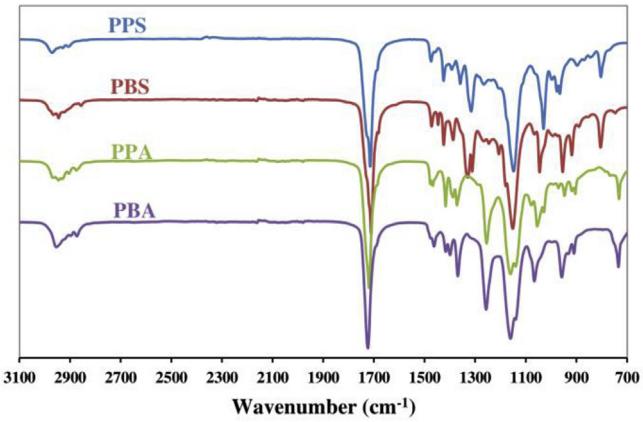

Fig. 3. FTIR spectra of PPS, PBS, PPA and PBA homopolyesters.

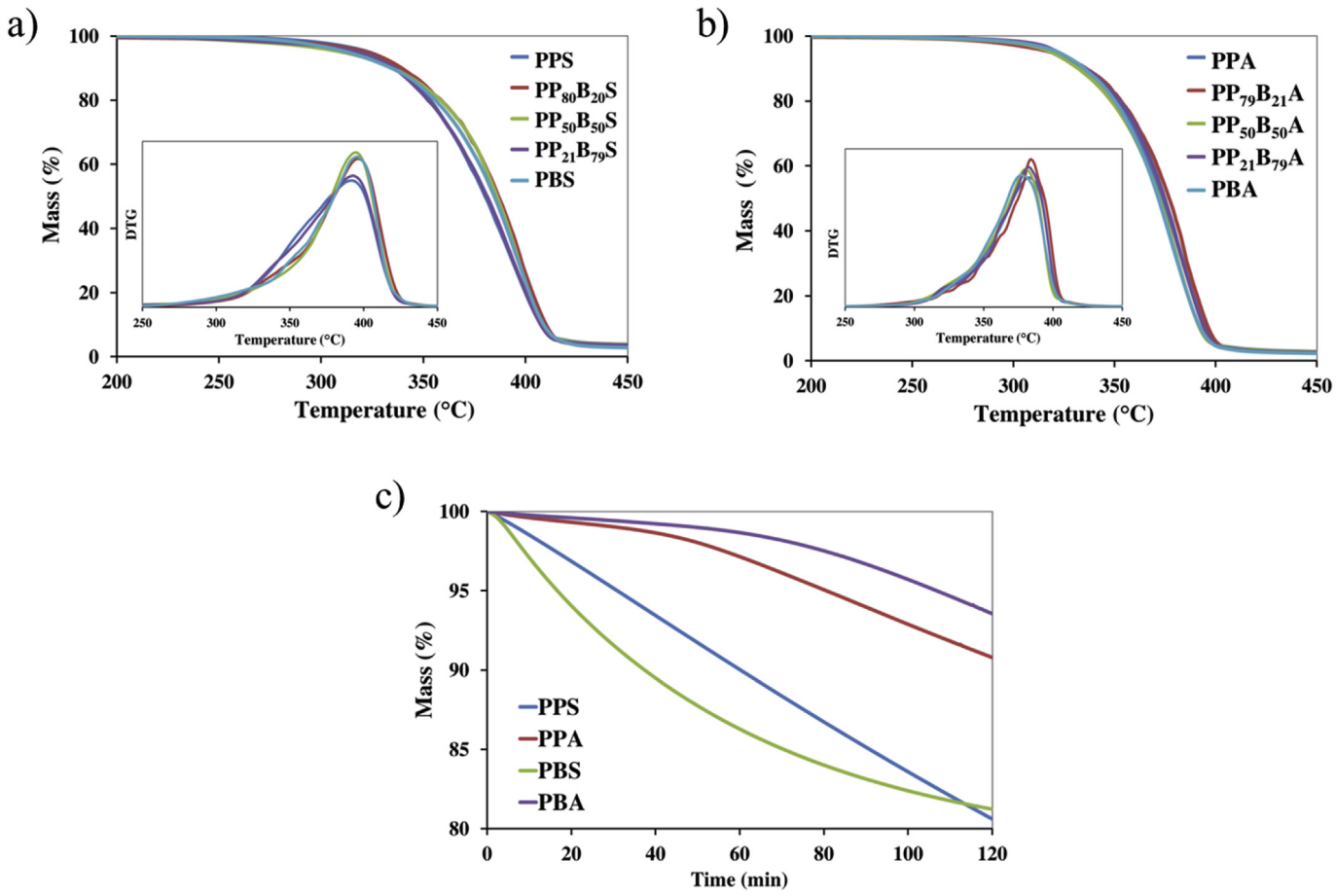

Fig. 4. Mass loss and DTG curves of (a) PPBS and (b) PPBA copolyesters under helium; (c) Isothermal mass loss curves of PPS, PPA, PBS and PBA homopolyesters at 230 °C under helium.

(90–95 wt%) occurred at 315–415 °C or 325–400 °C corresponding to the main degradation of PPBS and PPBA copolyesters, respectively [44]. At the end, a small amount of ashes (1–2 wt%) was recovered at 550 °C. The 2 wt% degradation temperature ($T_{d,2\%}$) of all PPBS and PPBA copolyesters were about 275–300 °C and 295–310 °C, respectively (Fig. 4-a,b). The 50 wt% degradation temperature ($T_{d,50\%}$) and the maximal degradation rate temperature ($T_{deg,max}$) were equivalent for all PPBS compositions (around 385 and 395 °C, respectively), leading to a similar degradation profile for all PPBS samples which were perfectly superimposed. The same tendency was observed for PPBA with $T_{d,50\%}$ and $T_{deg,max}$ of about 375 and 380 °C, respectively.

Isothermal mass loss curves at 230 °C (*i.e.*, corresponding to the polymerization reaction temperature) of the four homopolyesters are presented in Fig. 4-c. This isothermal degradation after 2 h was more important for succinate-based (~18 wt%) than adipate-based homopolyesters (~7–9 wt%). Moreover, the degradation profile varied strongly according to the homopolyester. As an example, PPS showed an important linear degradation, whereas PBS exhibited a non-linear degradation with a reduction of the mass loss rate with time. Both degradations seemed to be driven by only one mechanism of degradation. Finally, both adipate-based homopolyesters (*i.e.*, PPA and PBA) presented isothermal degradation profiles composed of two linear segments with an increase of the degradation rate after 40–60 min. One can suppose the presence of two mechanisms for these adipate-based homopolyesters, the first one at the beginning of the thermal degradation and the second one after the thermal degradation initiation.

The comparison of thermal degradation profile between PBS and PBA homopolyesters (representative of PPBS and PPBA copolyesters) (Table SI2), the isothermal degradation of the four homopolyesters and the use of $T_{d,2\%}$ as criterion for the thermal stability of polyesters all showed that adipate-based copolyesters possessed a higher thermal stability than succinate ones. As for the thermal stability, the degradation profile ($T_{d,50\%}$ and $T_{deg,max}$) depended exclusively on the carboxylic acid with a sharper degradation profile after the initiation for adipate-based copolyesters (Fig. 4-a,b) [13].

3.2.1. Crystalline structures

The crystalline structure of both copolyesters series was studied by WAXS. WAXS patterns of PPBS and PPBA copolyesters are shown in Fig. 5. PPBS WAXS patterns highlighted that all samples were semi-crystalline at room temperature and presented only one type of crystals by composition. First, main diffraction peaks of PBS appeared at 2θ = 19.4, 21.7 and 22.4°, whereas ones of PPS appeared at 2θ = 17.9, 19.4, 20.3 and 22.3°, in agreement with previous reports [13,22,29]. Then, PPBS copolyesters could be split into two groups according to the 1,3-PDO content. Indeed, PPBS containing 60 mol.% or less of 1,3-PDO units are characterized by WAXS patterns very similar to PBS, indicating that these copolyesters crystallized according to the PBS lattice and the comonomer (1,3-PDO in this case) incorporated in minor amount was excluded from the PBS crystals or only partially integrated in it.

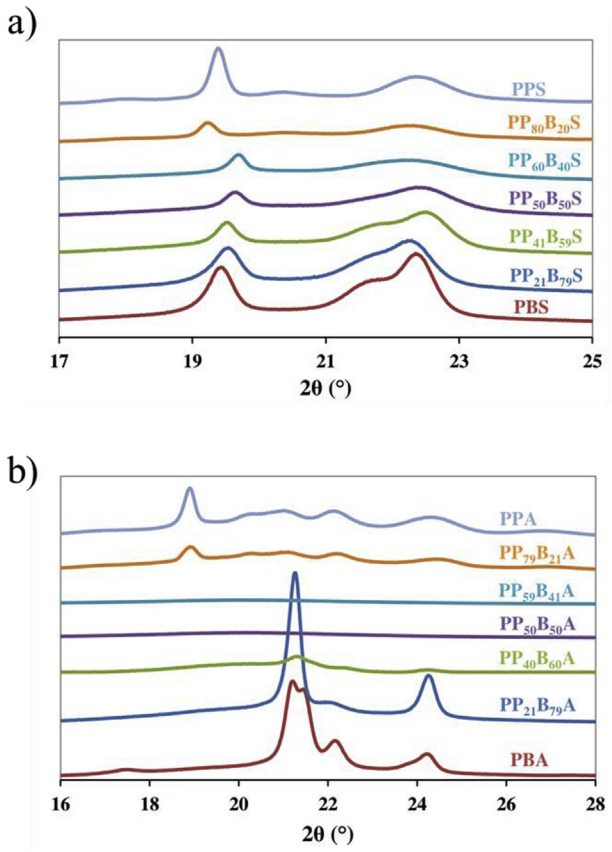

Fig. 5. WAXS patterns of (a) PPBS and (b) PPBA copolyesters and their parent homopolymers.

This led to the decrease of the crystal stability due to the presence of "defects" inside the chain and, thus, the degree of crystallinity decreased with the 1,3-PDO content. Moreover, one can observe that diffraction peaks broadened with the incorporation of the co-monomeric unit suggesting the decrease of the crystal size. On the contrary, samples containing 80 mol.% or more of 1,3-PDO units crystallized according to the PPS lattice.

Results from PPBA WAXS patterns indicated that, first, only some compositions were semi-crystalline at room temperature, since $PP_{50}B_{50}A$ and $PP_{59}B_{41}A$ were in molten state (see DSC analyses). On one side, PPA showed reflections at $2\theta = 18.9$, 20.2, 21.0, 22.1 and 24.3°. $PP_{79}B_{21}A$ with also BA units as minor component possessed only PPA type crystals but the diffraction peaks are less intense than for PPA due to the lower degree of crystallinity. On the other side, PPBA copolyesters with a 1,3-PDO content of 40 mol.% or lower exhibited WAXS patterns close to the one of PBA. PBA exhibited reflections at $2\theta = 21.2$ and 24.3° assigned to β-form crystals, but also reflections at $2\theta = 21.5$, 22.1 and 23.9° assigned to α-form crystals. The PBA homopolyester also exhibited α + β mixed crystals [45]. Such as for PBSA copolyesters, adipate-rich PPBA copolyesters (*i.e.*, $PP_{21}B_{79}A$ and $PP_{40}B_{60}A$) exhibited only β-form (kinetically favored) crystals of PBA, due to reduction of the crystallization rate by the inclusion of 1,3-PDO units [13].

3.2.2. Thermal behavior of copolyesters

Not only the thermal properties but also the crystalline structure of the copolyesters was studied by DSC, in complement to WAXS analysis. The cooling and second heating runs of (co)polyesters at 10 °C/min are presented in Fig. 6, whereas corresponding data are summarized in Table 2. The variation of thermal properties is discussed as a function of the ester function density (D_{ester}) calculated according to Equation (2).

During the first heating run, all copolyesters except $PP_{80}B_{20}A$ and $PP_{60}B_{40}A$ exhibited an endothermic peak associated to the fusion. The evolution of melting temperatures (T_m) and enthalpies (ΔH_m) of PPBS as a function of the 1,3-PDO content during the first heating run is presented in Fig. SI10-a. One can observe that T_m decreased from 116 to 32 °C with the 1,3-PDO content from PBS to $PP_{60}B_{40}S$, respectively, and then increased until 50 °C for PPS. Similarly, ΔH_m decreased with the inclusion of 1,3-PDO from 82 to 35 J/g for PBS to $PP_{80}B_{20}S$, respectively, and then increased until 46 J/g for PPS. T_m and ΔH_m exhibited, thus, a pseudo-eutectic behavior with minimal values for 1,3-PDO content around 60–80 mol.%. In the case of PPBA (Fig. SI10-b), a 1,3-PDO content around 50–60 mol.% led to molten state copolyesters at room temperature. Beyond these compositions, T_m and ΔH_m of PPBA copolyesters increased until having maximal values for 1,3-PDO content of 0 and 100 mol.% (*i.e.*, 58 °C and 80 J/g for PBA; 48 °C and 63 J/g for PPA). Since WAXS results evidenced only one crystal type by sample, the degree of crystallinity (X_c) of copolyesters was calculated according to Equation (1) using the homopolyesters ΔH_m° values determined from the groups contribution method of Van Krevelen [46] (124 and 135 J/g for PPA and PBA, respectively) or from experimental data [47] (140 and 210 J/g for PPS and PBS, respectively). Results are presented in Table 2. As observed by WAXS, the addition of a co-monomer to a homopolyester disrupted the symmetry of the chain and thus resulted in lower X_c for the copolyesters. Moreover, the increase of D_{ester} for homopolyesters resulted in a decrease of X_c from 59 (PBA) to 33% (PPS) due to the lower chain mobility. Indeed, D_{ester} increased with the amount of 1,3-PDO and SA unit in the copolyester.

During the cooling run, PPBS and PPBA copolyesters with 1,3-PDO content higher than 50 mol.% were not able to crystallize at 10 °C/min (Fig. 6-a,b), surely due to the presence of a high 1,3-PDO content decreasing the crystallization rate. Moreover, one can observe that, surprisingly, $PP_{41}B_{59}S$ crystallized less than $PP_{50}B_{50}S$ during the cooling. However, by decreasing the cooling rate to 5 °C/min, PPA and $PP_{59}B_{41}A$ were able to crystallize partially contrary to their PPBS counterpart (Figs. SI11 and SI.12). This last result highlighted the higher crystallization rate of copolyesters based on AA compared to those based on SA due to the increased chain mobility with the decrease of D_{ester}. $PP_{79}B_{21}A$ was also the only sample having an amorphous state after the cooling at 5 °C/min showing that the 79/21 (1,3-PDO/1,4-BDO) composition is the one with the lowest crystallization rate. Finally, for both copolyesters, the crystallization temperature (T_c) decreased significantly by increasing the 1,3-PDO content and T_c of PPBS copolyesters were globally higher than the one of PPBA.

The second heating run was characterized by the presence of a glass-transition phenomenon and a melting phenomenon. Moreover, $PP_{50}B_{50}S$, $PP_{41}B_{59}S$, PPA, $PP_{59}B_{41}A$ and $PP_{50}B_{50}A$ exhibited, in addition to these two phenomena, a cold-crystallization phenomenon due to an incomplete or the absence of the crystallization during the cooling run. PPA, despite its high 1,3-PDO content, is able to crystallize due to the absence of "BA" units "defects" in the chain structure, contrary to $PP_{79}B_{21}A$ which is amorphous.

Glass transition temperatures (T_g) of copolyesters, summarized in Table 2, are plotted in Fig. 7 as a function of the 1,3-PDO content. T_g of copolyesters increased with the 1,3-PDO content from −35 to −29 °C for PPBS and from −60 to −54 °C for PPBA. The decrease of the diol length of one carbon from 1,4-BDO to 1,3-PDO increases D_{ester}, which led to a higher amount of intra or inter-chain interactions between ester groups, hence the decrease of chain mobility leading to the increase of T_g. For the same reason, PPBA copolyesters containing "long" adipate segments had lower T_g than

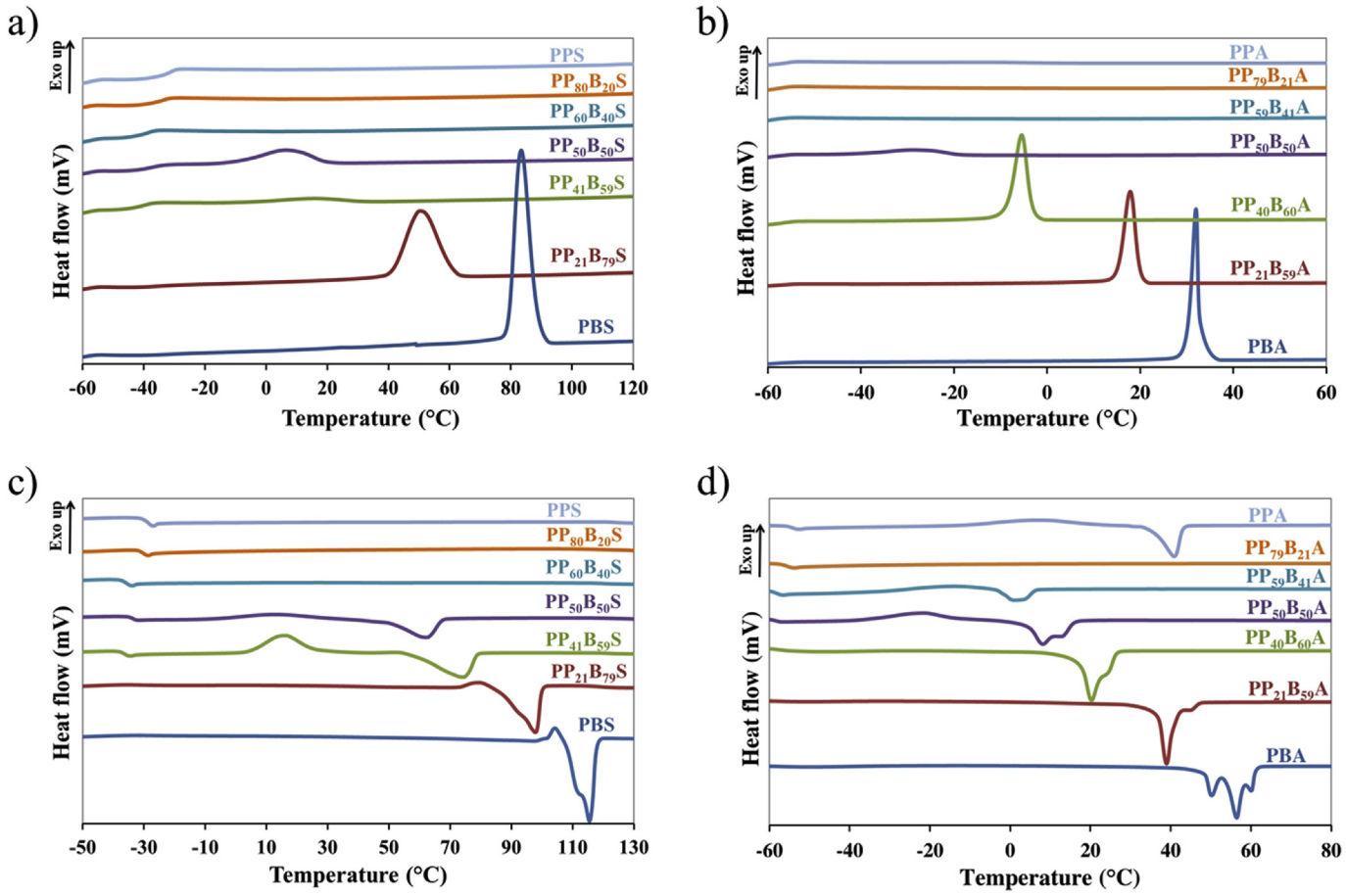

Fig. 6. DSC curves of the copolymers and the corresponding homopolymers. Cooling run curves of (a) PPBS and (b) PPBA; second heating run curves of (c) PPBS and (d) PPBA.

Table 2
DSC results of PPBS and PPBA copolyesters with heating and cooling rate of 10 °C/min.

Sample	D_{ester} %	First heating			Cooling		T_g[a] °C	Second heating				
		T_m °C	ΔH_m J/g	X_c %	T_c °C	ΔH_c J/g		T_{cc} °C	ΔH_{cc} J/g	T_m °C	ΔH_m J/g	X_c %
PPS	28.6	50	46	33	–	–	−29	–	–	–	–	–
$PP_{80}B_{20}S$	27.8	42	35	25	–	–	−31	–	–	–	–	–
$PP_{60}B_{40}S$	27.1	32	40	29	–	–	−33	–	–	–	–	–
$PP_{50}B_{50}S$	26.8	51	42	20	6	14	−33	14	5	62	28	13
$PP_{41}B_{39}S$	26.5	75	49	24	24	4	−35	16	31	74	39	19
$PP_{21}B_{79}S$	25.8	98	65	31	50	52	−34	–	–	98	52	25
PBS	25.0	116	82	39	83	67	−35	–	–	116	65	31
PPA	22.2	48	63	51	–	–	−54	7	25	41	29	23
$PP_{79}B_{21}A$	21.7	40	35	28	–	–	−56	–	–	–	–	–
$PP_{59}B_{41}A$	21.3	–	–	–	–	–	−58	−15	12	1	11	–
$PP_{50}B_{50}A$	21.1	–	–	–	−29	11	−57	−27	19	7	35	–
$PP_{40}B_{60}A$	20.9	33	29	21	−5	36	−58	–	–	20	36	27
$PP_{21}B_{79}A$	20.5	48	53	39	18	48	−59	–	–	40	47	35
PBA	20.0	58	80	59	32	55	−60	–	–	57	52	39

[a] T_g values were determined after a quenching from the melt.

PPBS copolyesters. For random copolyesters, the variation of T_g with the composition often follows the Fox equation [48], defined by Equation (4),

$$\frac{1}{T_{g,copo}} = \frac{w_1}{T_{g,1}} + \frac{w_2}{T_{g,2}} \quad (4)$$

where $T_{g,1}$ and $T_{g,2}$ are the glass transition temperature of homopolyesters, and w_1 and w_2 their respective mass fractions. One can observe, in Fig. 7-a, that the Fox equation did not fit well with our experimental data for PPBS, which seems in contradiction with the study of Papageorgiou and Bikiaris [29]. Nevertheless, the Fox equation fitted quite correctly with experimental data for PPBA (except for $PP_{59}B_{41}A$). However, sometimes the Gordon-Taylor equation [49] permitted to describe better the T_g variation of random aliphatic copolyesters such as PBSA or PPSA [13,28,50],

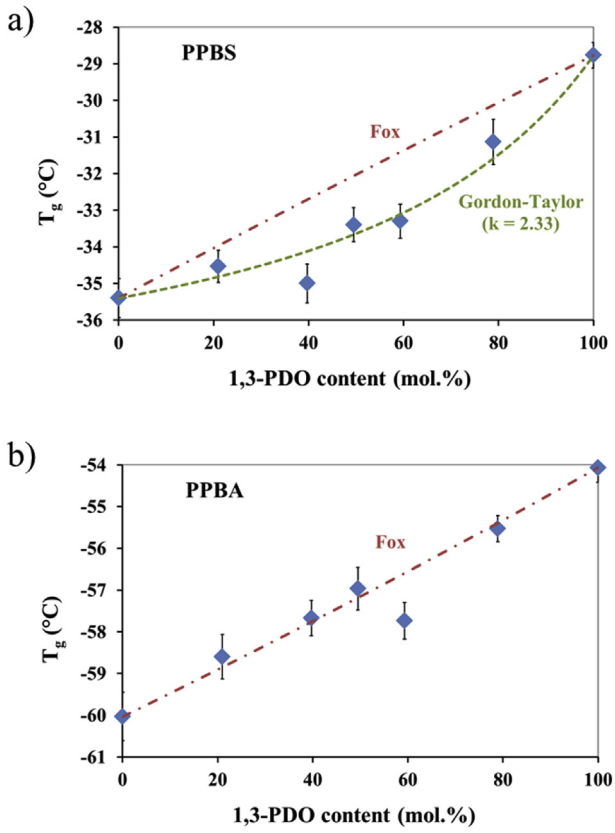

Fig. 7. Variation of the (a) PPBS and (b) PPBA experimental values of T_g *vs.* 1,3-PDO content in copolyesters and plots of theoretical Fox and Gordon-Taylor relations.

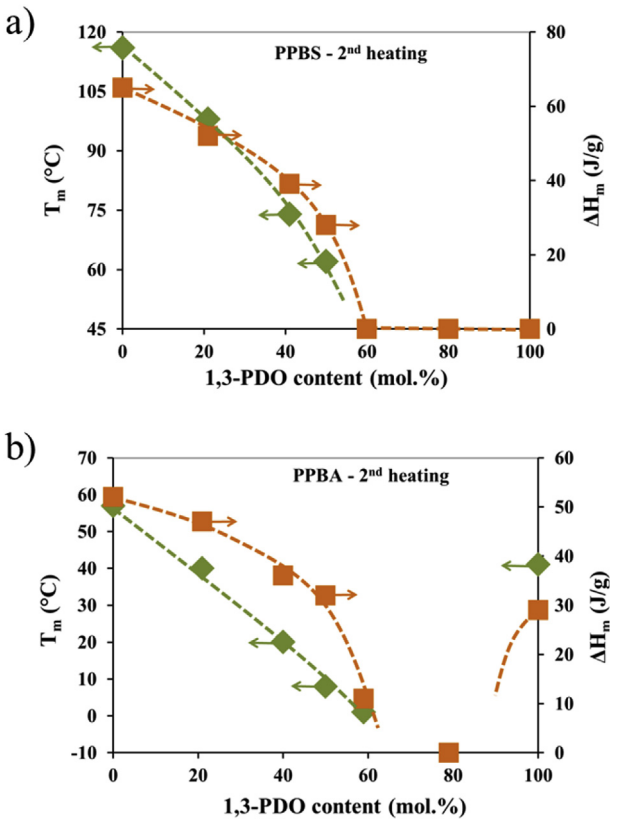

Fig. 8. Variation of T_m and ΔH_m *vs.* 1,3-PDO content for (a) PPBS and (b) PPBA during the second heating run.

which is defined by Equation (5),

$$T_{g,copo} = \frac{w_1\, T_{g,1} + k(1-w_1)\, T_{g,2}}{w_1 + k(1-w_1)} \quad (5)$$

where $T_{g,1}$ and $T_{g,2}$ are the glass transition temperature of homopolyesters, w_1 the respective mass fraction of the homopolyester 1 and k the Gordon-Taylor parameter. As observed in Fig. 7-a, the Gordon-Taylor equation fitted correctly our PPBS experimental data with k = 2.33. Usually k is considered as a fitting parameter [51], even if in the original version of volume additivity the parameter $k = \rho_l \Delta\alpha_2/\rho_2 \Delta\alpha_1$ was well defined (ρ_i is the density and $\Delta\alpha_i = \alpha_{melt} - \alpha_{glass}$ is the increment at T_g of the expansion coefficient of the respective component i). Nonetheless, the low amplitude of T_g values of PPBS and PPBA copolyesters decreases the accuracy of the mixing law differentiation for each copolyesters series and, thus, results should be taken with care.

Fig. 6-c,d highlighted that copolyesters exhibited crystallization-fusion phenomena composed of multiple peaks spread on large temperature ranges as commonly observed for aliphatic polyesters [12,13], due to the crystallite reorganization during the heating.

Plots of T_m and ΔH_m as a function of 1,3-PDO content of copolyesters during the second heating run are shown in Fig. 8. T_m and ΔH_m of PPBS decreased continuously with the 1,3-PDO content from 116 °C to 65 J/g for PBS until having an amorphous state for 1,3-PDO content higher than 50 mol.%. The incorporated co-monomeric unit (1,3-PDO in this case) was included in the PBS crystal lattice, disrupting its symmetry and, thus, decreasing the PBS crystal size and strength. According to WAXS results, only BS units were able to crystallize. The chemical structure of 1,3-PDO which has an odd and small number of methylene carbons was responsible for the poor crystallization rate of PPBS copolyesters containing high 1,3-PDO content. However, by reducing the heating rate to 5 °C/min, PPS, showed a small cold-crystallization phenomenon, thanks to the homogeneity of it structure (Fig. SI11). In the case of PPBA, only the composition with a 1,3-PDO content of 80 mol.% showed an amorphous behavior even at a heating rate of 5 °C/min (Fig. SI12). Indeed, Fig. 6-b,d showed that $PP_{59}B_{41}A$ and PPA, which are not able to crystallize at 10 °C/min during the cooling run, exhibited a small cold-crystallization phenomenon during the second heating run contrary to $PP_{60}B_{40}S$ and PPS confirming the better crystallization ability for copolyesters with AA compared to SA. As for PPBS, T_m and ΔH_m of PPBA decreased by increasing the 1,3-PDO content from 57 °C to 52 J/g for PBA until having an amorphous behavior for the composition with 80 mol.% of 1,3-PDO. However, PPA showed a semi-crystalline behavior with T_m at 41 °C and ΔH_m of 29 J/g, due to (i) the absence of "BA" units "defects" in the chain structure and (ii) the presence of AA segments (instead of SA segments) which increased the crystallization rate. X_c of copolyesters, determined from the second heating run, followed the trend of ΔH_m. However, one can observe that for an equivalent 1,3-PDO content, PPBA copolyesters had an higher X_c than PPBS proving the higher crystallization ability when increasing the diacid chain length from four to six carbons.

From DSC results showing (i) the presence of a pseudo-eutectic melting behavior for both copolyesters and (ii) that copolyester samples with low 1,3-PDO content are able to crystallize during the cooling run despite their randomness and from the WAXS results showing that (i) the minor co-monomeric units of one type are included in the crystal lattice of the other and vice versa, and (ii) crystalline unit cell parameters are composition dependent with

only one crystal type by sample switching from one unit cell to the other one around the pseudo-eutectic point, it can be concluded that PPBS and PPBA showed isodimorphic co-crystallization behavior, in agreement with previous results on aliphatic copolyesters [13,28,50,52].

3.3. Aerobic biodegradation in soil

An aerobic biodegradation of PPS, PBS, PPA, PBA and $PP_{50}B_{50}S$ samples was performed in soil to determine the influence of composition on the biodegradation rate. The cumulative CO_2 and percentage biodegradation profiles for each test sample are shown in Fig. 9. A steady rate of carbon dioxide evolution from each test vessel, similar to cellulose reference, indicated that test materials were metabolized by soil microorganisms and did not have any residual ecotoxicity effect (Fig. 9-a). Biodegradation of the reference material cellulose was initiated immediately after incubation in soil, without any lag phase, suggesting presence of actively metabolizing microbial population. Cellulose was 100% degraded within 60 days of incubation in soil (Fig. 9-b). In comparison, most test specimens had an initial lag phase (~3 days) and thereafter their biodegradation progressed slowly. An exception was test material PBS that showed a lag of almost two weeks before its degradation commenced. It is likely that the higher molar mass of PBS may be responsible for the longer lag phase. After 90 days of incubation in soil, PBA and PBS showed slightly higher degree of degradation (44% and 40%, respectively) as compared to PPA and PPS (35% and 40% respectively). As the time progressed, PBA and PBS continued to biodegrade at almost similar rate and achieved maximum biodegradation of 61% and 71% respectively at the end of 180 days (Fig. 9-b). In comparison, biodegradation profile of PPA and PPS plateaued, achieving a maximum biodegradation of 47% and 48%, respectively. $PP_{50}B_{50}S$ achieved a maximum biodegradation of 50% at the end of 6 months (*i.e.* 180 days). It has been reported that the degree of crystallinity or melting temperatures of samples are important factors for the biodegradation rate [53,54]. However, results obtained in this study did not show any correlation between these two factors and rate of biodegradation of different samples. Test results suggested that chemical structure of polyesters influenced the biodegradation rate, which increased by increasing the length of the monomers. An increase in the diol chain length from 3 to 4 carbons led to a significant increase in the biodegradation rate, whereas the increase in the diacid chain length only had a minor effect on the biodegradation rate. These results suggested that lower ester function density of polyesters using AA instead of SA and 1,4-BDO instead of 1,3-PDO, allowing a higher chain flexibility attested by lower T_g values, permitted a higher degradation by microorganisms in soil. Nevertheless, the global ester function density is not the key parameter, strictly speaking, since calculated PPA ester function density was lower than the one of PBS. It is more likely that the key parameter that influenced degradation rate was rather the number of methylene carbons in monomers (*i.e.*, diacids and diols) between ester functions. Finally, since none of polyesters samples achieved a degree of biodegradation of 90% within 6 months, these samples cannot be considered as biocompostable according to the ISO 17556 regulation.

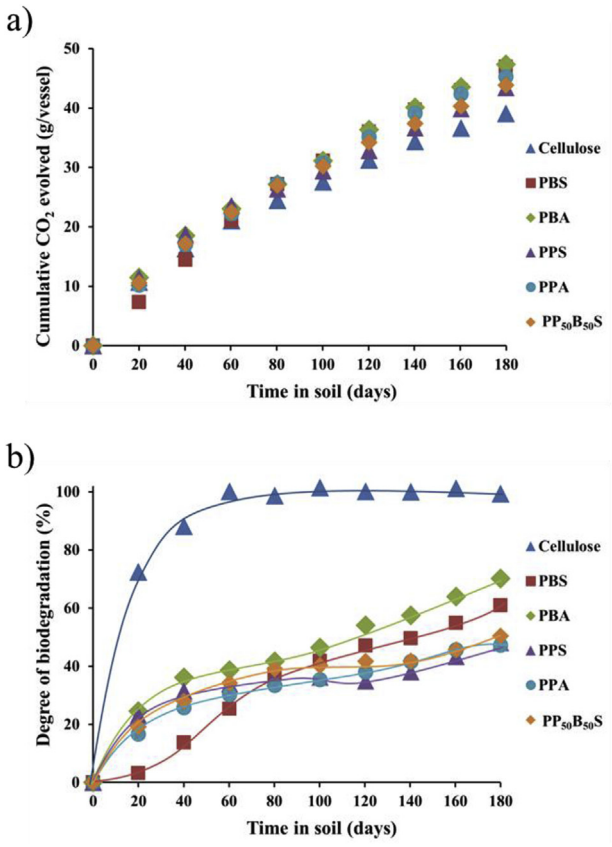

Fig. 9. Average values of (a) cumulative CO_2 data and (b) degree of biodegradation of reference (cellulose) and test materials as a function of degradation time in soil.

4. Conclusion

Two potentially biobased aliphatic copolyesters (PPBA and PPBS) based on renewable building blocks were successfully synthesized at different composition in melt with TTIP as catalyst. For both types of copolyesters, the synthetic pathway permitted to obtain (i) high molar masses, (ii) copolyesters with the same final molar composition than initial feed ratio and (iii) a random distribution between 1,3-PDO and 1,4-BDO segments along the (co) polyester chain.

PPBA and PPBS copolyesters exhibited both an excellent thermal stability without mass loss before 300 °C. Moreover, analysis of PPBS and PPBA copolyesters exhibited that the chemical nature and length of the diol had no effect on the thermal degradation profile unlike the diacid used.

Both copolyesters showed an isodimorphic co-crystallization behavior characterized by a pseudo-eutectic melting behavior and the presence of only one crystalline phase by sample, except for PPBA copolyesters with 1,3-PDO content of 50–59 mol.% which were in molten state at ambient temperature. The inclusion of the second co-monomer inside the crystal lattice altered significantly the crystal structures leading to a decrease of the degree of crystallinity with the co-monomer content. Moreover, the fact that some samples with high 1,3-PDO content did not crystallize during the cooling or the second heating run at a cooling/heating rate of 10 °C/min showed that 1,3-PDO decreased significantly the crystallization rate of the copolyesters. Finally, T_g of copolyesters increased with the 1,3-PDO content and by using SA instead of AA, due to the decrease of the chain mobility resulting from an increase of the ester function density.

One of the important features was that the aerobic biodegradation rate in soil increased slightly with the increase of the diol length from 3 to 4 carbons and especially with the diacid length from 4 to 6 carbons, without showing any residual ecotoxicity.

Finally, these two copolyesters seemed promising biobased and biodegradable materials, with the addition of 1,3-PDO units in the copolyesters being an interesting way to decrease their degree of

crystallinity. These materials could thus have suitable properties for applications such as short-term-packaging, especially PPBS copolyesters with low 1,3-PDO content, since it has close properties to PBS and PBSA, which are produced industrially and well known for their applications on biodegradable packaging. Copolyesters with high 1,3-PDO content would be more suitable for applications such as adhesives due to their low crystallinity. To complete this study and confirm such potential applications, further investigations for instance on the climatic ageing (effect of humidity, temperature, UV) and the gas barrier properties of these materials could be performed.

Acknowledgements

This work has received funding from the European's Union 7th Framework Program for research, technological development and demonstration under grant agreement n°311815 (SYNPOL Project). In addition, the authors are grateful to the BioAmber company for the supply of Bio-succinic acid.

Appendix A. Supplementary data

Supplementary data related to this chapter can be found at http://dx.doi.org/10.1016/j.polymer.2017.06.045.

References

[1] C. Vilela, A.F. Sousa, A.C. Fonseca, A.C. Serra, J.F.J. Coelho, C.S.R. Freire, A.J.D. Silvestre, The quest for sustainable polyesters – insights into the future, Polym. Chem. 5 (2014) 3119–3141, http://dx.doi.org/10.1039/C3PY01213A.
[2] E. Pollet, L. Avérous, Production, chemistry and properties of polyhydroxyalkanoates, in: D. Plackett (Ed.), Biopolym. – New Mater. Sustain. Films Coat, John Wiley & Sons, Ltd, Chichester, 2011, pp. 65–86 (accessed February 16, 2016), http://onlinelibrary.wiley.com/doi/10.1002/9781119994312.ch4/summary.
[3] L. Avérous, Biodegradable multiphase systems based on plasticized starch: a review, J. Macromol. Sci. Part C 44 (2004) 231–274, http://dx.doi.org/10.1081/MC-200029326.
[4] M. Gigli, M. Fabbri, N. Lotti, R. Gamberini, B. Rimini, A. Munari, Poly(butylene succinate)-based polyesters for biomedical applications: a review, Eur. Polym. J. 75 (2016) 431–460, http://dx.doi.org/10.1016/j.eurpolymj.2016.01.016.
[5] H. Biebl, K. Menzel, A.-P. Zeng, W.-D. Deckwer, Microbial production of 1,3-propanediol, Appl. Microbiol. Biotechnol. 52 (1999) 289–297, http://dx.doi.org/10.1007/s002530051523.
[6] A. Drożdżyńska, K. Leja, K. Czaczyk, Biotechnological production of 1,3-propanediol from crude glycerol, BioTechnologia 1 (2011) 92–100, http://dx.doi.org/10.5114/bta.2011.46521.
[7] J.J. Bozell, G.R. Petersen, Technology development for the production of biobased products from biorefinery carbohydrates—the US Department of Energy's "Top 10" revisited, Green Chem. 12 (2010) 539–554, http://dx.doi.org/10.1039/b922014c.
[8] J. Becker, A. Lange, J. Fabarius, C. Wittmann, Top value platform chemicals: bio-based production of organic acids, Curr. Opin. Biotechnol. 36 (2015) 168–175, http://dx.doi.org/10.1016/j.copbio.2015.08.022.
[9] I. Bechthold, K. Bretz, S. Kabasci, R. Kopitzky, A. Springer, Succinic acid: a new platform chemical for biobased polymers from renewable resources, Chem. Eng. Technol. 31 (2008) 647–654, http://dx.doi.org/10.1002/ceat.200800063.
[10] N.R. Barton, A.P. Burgard, M.J. Burk, J.S. Crater, R.E. Osterhout, P. Pharkya, B.A. Steer, J. Sun, J.D. Trawick, S.J.V. Dien, T.H. Yang, H. Yim, An integrated biotechnology platform for developing sustainable chemical processes, J. Ind. Microbiol. Biotechnol. 42 (2014) 349–360, http://dx.doi.org/10.1007/s10295-014-1541-1.
[11] M. Reulier, L. Avérous, Elaboration, morphology and properties of renewable thermoplastics blends, based on polyamide and polyurethane synthesized from dimer fatty acids, Eur. Polym. J. 67 (2015) 418–427, http://dx.doi.org/10.1016/j.eurpolymj.2014.11.036.
[12] T. Debuissy, E. Pollet, L. Avérous, Synthesis of potentially biobased copolyesters based on adipic acid and butanediols: kinetic study between 1,4- and 2,3-butanediol and their influence on crystallization and thermal properties, Polymer 99 (2016) 204–213, http://dx.doi.org/10.1016/j.polymer.2016.07.022.
[13] T. Debuissy, E. Pollet, L. Avérous, Synthesis and characterization of biobased poly(butylene succinate-ran-butylene adipate). Analysis of the composition-dependent physicochemical properties, Eur. Polym. J. 87 (2017) 84–98, http://dx.doi.org/10.1016/j.eurpolymj.2016.12.012.
[14] T.A. Werpy, J.E. Holladay, J.F. White, Top value added chemicals from biomass: I. Results of screening for potential candidates from sugars and synthesis gas, pacific northwest national laboratory (pnnl), richland, wa (US) (accessed March 23, 2016), https://www.osti.gov/scitech/biblio/926125-top-value-added-chemicals-from-biomass-results-screening-potential-candidates-from-sugars-synthesis-gas, 2004.
[15] T. Debuissy, E. Pollet, L. Avérous, Titanium-catalyzed transesterification as a route to the synthesis of fully biobased poly(3-hydroxybutyurate-co-butylene dicarboxylate) copolyesters, from their homopolyesters, Eur. Polym. J. 90 (2017) 92–104, http://dx.doi.org/10.1016/j.eurpolymj.2017.03.006.
[16] T. Polen, M. Spelberg, M. Bott, Toward biotechnological production of adipic acid and precursors from biorenewables, J. Biotechnol. 167 (2013) 75–84, http://dx.doi.org/10.1016/j.jbiotec.2012.07.008.
[17] S. Luo, F. Li, J. Yu, A. Cao, Synthesis of poly(butylene succinate-co-butylene terephthalate) (PBST) copolyesters with high molecular weights via direct esterification and polycondensation, J. Appl. Polym. Sci. 115 (2010) 2203–2211, http://dx.doi.org/10.1002/app.31346.
[18] J. Xu, B.-H. Guo, Poly(butylene succinate) and its copolymers: research, development and industrialization, Biotechnol. J. 5 (2010) 1149–1163, http://dx.doi.org/10.1002/biot.201000136.
[19] R.-M. Ho, K.-Z. Ke, M. Chen, Crystal structure and banded spherulite of poly(trimethylene terephthalate), Macromolecules 33 (2000) 7529–7537, http://dx.doi.org/10.1021/ma000210w.
[20] B. Wang, C.Y. Li, J. Hanzlicek, S.Z.D. Cheng, P.H. Geil, J. Grebowicz, R.-M. Ho, Poly(trimethylene teraphthalate) crystal structure and morphology in different length scales, Polymer 42 (2001) 7171–7180, http://dx.doi.org/10.1016/S0032-3861(01)00046-5.
[21] I.M. Ward, M.A. Wilding, H. Brody, The mechanical properties and structure of poly(m-methylene terephthalate) fibers, J. Polym. Sci. Polym. Phys. Ed. 14 (1976) 263–274, http://dx.doi.org/10.1002/pol.1976.180140206.
[22] M. Soccio, N. Lotti, L. Finelli, M. Gazzano, A. Munari, Aliphatic poly(propylene dicarboxylate)s: effect of chain length on thermal properties and crystallization kinetics, Polymer 48 (2007) 3125–3136, http://dx.doi.org/10.1016/j.polymer.2007.04.007.
[23] D.N. Bikiaris, G.Z. Papageorgiou, D.J. Giliopoulos, C.A. Stergiou, Correlation between chemical and solid-state structures and enzymatic hydrolysis in novel biodegradable polyesters. The case of poly(propylene alkanedicarboxylate)s, Macromol. Biosci. 8 (2008) 728–740, http://dx.doi.org/10.1002/mabi.200800035.
[24] S.S. Umare, A.S. Chandure, R.A. Pandey, Synthesis, characterization and biodegradable studies of 1,3-propanediol based polyesters, Polym. Degrad. Stab. 92 (2007) 464–479, http://dx.doi.org/10.1016/j.polymdegradstab.2006.10.007.
[25] G.Z. Papageorgiou, D.N. Bikiaris, Crystallization and melting behavior of three biodegradable poly(alkylene succinates). A comparative study, Polymer 46 (2005) 12081–12092, http://dx.doi.org/10.1016/j.polymer.2005.10.073.
[26] S.G. Nanaki, K. Pantopoulos, D.N. Bikiaris, Synthesis of biocompatible poly(ε-caprolactone)- block-poly(propylene adipate) copolymers appropriate for drug nanoencapsulation in the form of core-shell nanoparticles, Int. J. Nanomedicine 6 (2011) 2981–2995, http://dx.doi.org/10.2147/IJN.S26568.
[27] G.Z. Papageorgiou, D.N. Bikiaris, Synthesis and properties of novel biodegradable/biocompatible poly[propylene-co-(ethylene succinate)] random copolyesters, Macromol. Chem. Phys. 210 (2009) 1408–1421, http://dx.doi.org/10.1002/macp.200900132.
[28] T. Debuissy, E. Pollet, L. Avérous, Synthesis and characterization of fully biobased poly(propylene succinate-ran-propylene adipate). Analysis of the architecture-dependent physicochemical behavior, J. Polym. Sci. Part Polym. Chem. (2017), http://dx.doi.org/10.1002/pola.28668 n/a-n/a.
[29] G.Z. Papageorgiou, D.N. Bikiaris, Synthesis, cocrystallization, and enzymatic degradation of novel poly(butylene-co-propylene succinate) copolymers, Biomacromolecules 8 (2007) 2437–2449, http://dx.doi.org/10.1021/bm0703113.
[30] Y. Xu, J. Xu, B. Guo, X. Xie, Crystallization kinetics and morphology of biodegradable poly(butylene succinate-co-propylene succinate)s, J. Polym. Sci. Part B Polym. Phys. 45 (2007) 420–428, http://dx.doi.org/10.1002/polb.20877.
[31] Y. Xu, J. Xu, D. Liu, B. Guo, X. Xie, Synthesis and characterization of biodegradable poly(butylene succinate-co-propylene succinate)s, J. Appl. Polym. Sci. 109 (2008) 1881–1889, http://dx.doi.org/10.1002/app.24544.
[32] S.-F. Lu, M. Chen, Y.-C. Shih, C.H. Chen, Nonisothermal crystallization kinetics of biodegradable poly(butylene succinate-co-propylene succinate)s, J. Polym. Sci. Part B Polym. Phys. 48 (2010) 1299–1308, http://dx.doi.org/10.1002/polb.22027.
[33] S.-F. Lu, M. Chen, C.H. Chen, Mechanisms and kinetics of thermal degradation of poly(butylene succinate-co-propylene succinate)s, J. Appl. Polym. Sci. 123 (2012) 3610–3619, http://dx.doi.org/10.1002/app.34999.
[34] C.-H. Chen, J.-S. Peng, M. Chen, H.-Y. Lu, C.-J. Tsai, C.-S. Yang, Synthesis and characterization of poly(butylene succinate) and its copolyesters containing minor amounts of propylene succinate, Colloid Polym. Sci. 288 (2010) 731–738, http://dx.doi.org/10.1007/s00396-010-2187-9.
[35] I. Arandia, A. Mugica, M. Zubitur, A. Arbe, G. Liu, D. Wang, R. Mincheva, P. Dubois, A.J. Müller, How composition determines the properties of isodimorphic poly(butylene succinate-ran-butylene azelate) random biobased copolymers: from single to double crystalline random copolymers, Macromolecules 48 (2015) 43–57, http://dx.doi.org/10.1021/ma5023567.
[36] A. Díaz, L. Franco, J. Puiggalí, Study on the crystallization of poly(butylene azelate-co-butylene succinate) copolymers, Thermochim. Acta 575 (2014)

45–54, http://dx.doi.org/10.1016/j.tca.2013.10.013.
[37] A. Spyros, D.S. Argyropoulos, R.H. Marchessault, A study of poly(-hydroxyalkanoate)s by quantitative 31P NMR Spectroscopy: molecular weight and chain cleavage, Macromolecules 30 (1997) 327–329, http://dx.doi.org/10.1021/ma9601979.
[38] C. Way, D.Y. Wu, K. Dean, E. Palombo, Design considerations for high-temperature respirometric biodegradation of polymers in compost, Polym. Test. 29 (2010) 147–157, http://dx.doi.org/10.1016/j.polymertesting.2009.10.004.
[39] C.-T. Kuo, S.-A. Chen, Kinetics of polyesterification: adipic acid with ethylene glycol, 1,4-butanediol, and 1,6-hexanediol, J. Polym. Sci. Part Polym. Chem. 27 (1989) 2793–2803, http://dx.doi.org/10.1002/pola.1989.080270823.
[40] R. Yamadera, M. Murano, The determination of randomness in copolyesters by high resolution nuclear magnetic resonance, J. Polym. Sci. [A1] 5 (1967) 2259–2268, http://dx.doi.org/10.1002/pol.1967.150050905.
[41] P. Korntner, I. Sumerskii, M. Bacher, T. Rosenau, A. Potthast, Characterization of technical lignins by NMR spectroscopy: optimization of functional group analysis by 31P NMR spectroscopy, Holzforschung 69 (2015) 807–814, http://dx.doi.org/10.1515/hf-2014-0281.
[42] Q. Charlier, E. Girard, F. Freyermouth, M. Vandesteene, N. Jacquel, C. Ladavière, A. Rousseau, F. Fenouillot, Solution viscosity – molar mass relationships for poly(butylene succinate) and discussion on molar mass analysis, Express Polym. Lett. 9 (2015) 424–434, http://dx.doi.org/10.3144/expresspolymlett.2015.41.
[43] A. Munari, P. Manaresi, E. Chiorboli, A. Chiolle, Dilute solution properties of poly(butylene adipate) and poly(butylene adipate-co-butylene isophthalate), Eur. Polym. J. 28 (1992) 101–106, http://dx.doi.org/10.1016/0014-3057(92)90244-V.
[44] T. Debuissy, E. Pollet, L. Avérous, Enzymatic synthesis of a bio-based copolyester from poly(butylene succinate) and poly((r)-3-hydroxybutyrate): study of reaction parameters on the transesterification rate, Biomacromolecules 17 (2016) 4054–4063, http://dx.doi.org/10.1021/acs.biomac.6b01494.
[45] P. Pan, Y. Inoue, Polymorphism and isomorphism in biodegradable polyesters, Prog. Polym. Sci. 34 (2009) 605–640, http://dx.doi.org/10.1016/j.progpolymsci.2009.01.003.
[46] D.W. Van Krevelen, Chapter 5-Calorimetric properties, in: Prop. Polym. Third Complet. Revis. Ed, Elsevier, Amsterdam, 1997, pp. 109–127 (accessed March 8, 2016), http://www.sciencedirect.com/science/article/pii/B9780444828774500123.
[47] G.Z. Papageorgiou, D.N. Bikiaris, Crystallization and melting behavior of three biodegradable poly(alkylene succinates). A comparative study, Polymer 46 (2005) 12081–12092, http://dx.doi.org/10.1016/j.polymer.2005.10.073.
[48] T. Fox, Influence of diluent and of copolymer composition on the glass temperature of a polymer system, Bull. Am. Phys. Soc. 1 (1956) 123–132.
[49] M. Gordon, J.S. Taylor, Ideal copolymers and the second-order transitions of synthetic rubbers. i. non-crystalline copolymers, J. Appl. Chem. 2 (2007) 493–500, http://dx.doi.org/10.1002/jctb.5010020901.
[50] R.A. Pérez-Camargo, B. Fernández-d'Arlas, D. Cavallo, T. Debuissy, E. Pollet, L. Avérous, A.J. Müller, Tailoring the structure, morphology, and crystallization of isodimorphic poly(butylene succinate-ran-butylene adipate) random copolymers by changing composition and thermal history, Macromolecules 50 (2017) 597–608, http://dx.doi.org/10.1021/acs.macromol.6b02457.
[51] E. Penzel, J. Rieger, H.A. Schneider, The glass transition temperature of random copolymers: 1. Experimental data and the Gordon-Taylor equation, Polymer 38 (1997) 325–337, http://dx.doi.org/10.1016/S0032-3861(96)00521-6.
[52] R.A. Pérez–Camargo, G. Saenz, S. Laurichesse, M.T. Casas, J. Puiggalí, L. Avérous, A.J. Müller, Nucleation, crystallization, and thermal fractionation of poly (ε-Caprolactone)-Grafted-Lignin: effects of grafted chains length and lignin content, J. Polym. Sci. Part B Polym. Phys. 53 (2015) 1736–1750, http://dx.doi.org/10.1002/polb.23897.
[53] J. Šerá, P. Stloukal, P. Jančová, V. Verney, S. Pekařová, M. Koutný, Accelerated biodegradation of agriculture film based on aromatic–aliphatic copolyester in soil under mesophilic conditions, J. Agric. Food Chem. 64 (2016) 5653–5661, http://dx.doi.org/10.1021/acs.jafc.6b01786.
[54] P. Rizzarelli, M. Cirica, G. Pastorelli, C. Puglisi, G. Valenti, Aliphatic poly(ester amide)s from sebacic acid and aminoalcohols of different chain length: synthesis, characterization and soil burial degradation, Polym. Degrad. Stab. 121 (2015) 90–99, http://dx.doi.org/10.1016/j.polymdegradstab.2015.08.010.